Eur Radiol (2010) 20: 2491–2495
DOI 10.1007/s00330-010-1815-6

NEURO

Maria Isabel Vargas
Duy Nguyen
Magalie Viallon
Zolt Kulcsár
Enrico Tessitore
Benedict Rilliet
Daniel Rufenacht
Karl Lovblad

Dynamic MR angiography (MRA) of spinal vascular diseases at 3T

Received: 2 February 2010
Revised: 7 April 2010
Accepted: 13 April 2010
Published online: 16 May 2010

M. I. Vargas (✉) · D. Nguyen · K. Lovblad
Department of Neuroradiology, DISIM,
Geneva University Hospital,
4 Gabrielle-Perret-Gentil, 1211, Genève 14,
Switzerland
e-mail: maria.i.vargas@hcuge.ch
Tel.: +41-22-3723775
Fax: +41-22-3727072

M. Viallon
Department of Radiology,
Geneva University Hospital, Geneva,
Switzerland

Z. Kulcsár · D. Rufenacht
Klinik Hirslanden, Neurozentrum,
Zurich, Switzerland

E. Tessitore · B. Rilliet
Department of Neurosurgery,
Geneva University Hospital, Geneva,
Switzerland

Abstract Spinal magnetic resonance angiography (MRA) is difficult to perform because of the size of the spinal cord vessels. High-field MR improves resolution and imaging speed. We examined 17 patients with spinal vascular diseases with dynamic contrast-enhanced three-dimensional MR sequences. In three patients, the artery of Adamkievicz could be seen; we could also detect all arteriovenous malformations and dural fistulas. MRA has the potential to replace diagnostic spinal angiography and the latter should be used only for therapeutic purposes.

Keywords Dynamic MR angiography · Spinal vascular malformations · Dural fistula · Arteriovenous malformation · Adamkievickz artery

Introduction

The small size of the structures in the spine [spinal cord 10–12 mm of diameter, spinal anterior artery 0.2–0.8 mm, Adamkievicz artery (AKA) 05–1.0 mm] [1, 2] makes it difficult to perform magnetic resonance angiographic (MRA) sequences in the spinal cord . The use of a higher magnetic field significantly improves the quality of images with a reduction in acquisition time [3]. This enables high resolution images of the different vascular phases (arterial, venous and late) to be obtained that are necessary for the study of the normal vessels and of vascular malformations in the spinal cord.

Materials and methods

We have examined 17 patients (for details see Table 1), eight female and nine male, aged 26–82 years, median age 52 years on a 3-Tesla MR system (Trio, Siemens, Forchheim, Germany); the patients were referred between January 2006 and October 2008 to the Department of Neuroradiology, Geneva University Hospital, with known spinal problems. The patients underwent the following imaging procedures after having been informed and according to our institutions guidelines. The protocol used was composed of sagittal T2-weighted imaging (T2WI) (TE 120, TR 3,500, 4-mm thickness, nine slices) and axial T2WI (TE 120, TR 4,000, 4-mm thickness, 20 slices), sagittal T1WI (TE 13, TR 626, 4-mm thickness, nine slices), diffusion tensor imaging (DTI) with 30 directions, three-dimensional (3D) MRA sequences (see details below) and fat-saturated T1WI in the sagittal (TE 12, TR 400, 4-mm thickness, nine slices) and axial (TE 12, TR 400, 4-mm thickness, 20 slices) planes after administration of contrast.

Three MRA acquisitions based on a 3D contrast enhanced gradient echo sequence were sequentially performed (Fig. 1) after a bolus injection of an intravascular contrast agent (0.2 mmol/kg, Vasovist; Bayer Schering, Berlin, Germany). The sequence was fat saturated and therefore it was not centrically reordered. A test bolus was then performed in order to determine the

Table 1 Patient imaging findings (*AKA* Adamkievicz artery, *AVM* arteriovenous malformation)

Sex	Age	Symptoms	MRA findings	MRI findings
M	50	Transient recurrent paraparesies	Localization AKA	None
F	30	Back pain	Localization AKA	Extradural cyst
F	75	Back pain	Localization AKA	Metastasis from colon carcinoma Th11–Th12
M	58	Progressive paraplegia	Dural fistula Th6 left	Hyperintensity Th5 of the spinal cord and dilatation of perimedullary vessels
M	57	Progressive paraplegia	Dural fistula Th9 right	Hyperintensity in the whole spinal cord associated with dilated perimedullary vessels
M	80	Progressive paraplegia and back pain	Dural fistula Th11 left	Hyperintensity in the dorsal segment and medullary cone associated a with dilated perimedullary vessels
F	70	Progressive paraplegia	Dural fistula Th6 left	Hyperintensity in the medullary cone with enhancement and slight dilatation of perimedullary vessels
F	26	Dysesthesia left superior extremity and motor deficit of the left leg	Cervical AVM	Dilated vessel and nidus in perimedullary right space associated with bone erosion
M	29	Motor deficit and spasticity of right inferior extremity	AVM Th4–Th6	Flow-voids in the spinal cord and dilated perimedullary vessels
M	50	Neck pain and paresthesias of both superior extremities	AVM C1–C3	Flow-voids in the spinal cord and dilated perimedullary vessels
F	41	Back pain and sudden paraplegia	None	Spinal cord cavernoma
M	57	Paresthesia of two lower extremities	Dilated vessels inside the mass	Epidural heterogeneous mass (hemangioma) at Th3–Th5 with flow voids inside and medullary compression
F	38	Paraparesis, constipation and bladder dysfunction	Dilated vessel around the masses and in the perimedullary space	Multiple hypervascular heterogeneous masses associated medullary compression and intramedullary hyperintensity (hemangioblastomas)
M	52	Sudden tetraplegia	None	Cervical spinal cord ischemia
F	82	Sudden paraplegia and bowel/bladder dysfunction	None	Medullary cone ischemia
F	60	Sudden paraplegia and bowel/bladder dysfunction	None	Medullary cone ischemia
M	73	Sudden paraplegia and bowel/bladder dysfunction	None	Medullary cone ischemia

arrival time of the contrast agent in the arteries feeding the spinal cord, and the acquisition was started adequately so that the acquisition of the k-space centre matched the bolus arrival time. For the arterial and venous 3D gradient echo MR sequence, the parameters were TE/TR/flip angle =1.52 ms/3.98 ms/20°, a matrix size of 384, pixel size= 1.2×1.0×0.9 mm, field of view (FOV)=380 mm, no rectangular FOV, 88 slices, 0.9-mm slice thickness, bandwidth (BW)=410 Hz/px. The phase encoding direction was chosen in the cranio-caudal direction to avoid flow and motion artefacts from the ascending hyperintense aorta projecting on the spinal cord, with an additional 33% oversampling. The sequence was acquired at the isocentre and required 1 min for a single phase.

For the high resolution late enhanced 3D gradient echo MR sequence, the parameters were TE/TR/flip angle= 1.89 ms/4.95 ms/20°, two averages, a matrix size of 512, pixel size=0.7×0.6×0.6 mm, FOV=330 mm, no rectangular FOV, 72 slices, 0.6 mm slice thickness, BW= 410 Hz/px. The sequence was also performed systematically at the isocentre. MPR reformatting and thin MIP reconstructions were realized for all acquisitions.

All cases, with the exception of AKA localization and patients with ischemic lesions, had a conventional angiography. The tumours were proven by histology.

Results

In all patients the main spinal vessels were seen and abnormal vascular lesions were visualized (see Table 1).

In two out of three patients examined for localization of the AKA, the visualization was easily done (Fig. 2), whereas in the third patient differentiation between artery and vein was more difficult, but possible by performing maximum intensity projection (MIP) and multiplanar reconstruction (MPR).

In four cases of dural fistula the exact localization of the fistula was possible (Fig. 3).

In three cases with AVM, the level of malformation and the intra- and perimedullary localization was done as well as the arteries implicated (Fig. 4). The little shunts inside the nidus could not be individualized.

Cavernomas are not seen on MRA and on conventional angiography; therefore, the realization of angiographic sequences is not necessary. In tumours such as hemangiomas or hemangioblastomas, hypervascularization was detected in addition to morphology and location of the masses.

In ischaemia [4], the parenchymal anomalies were visible early on diffusion imaging but unfortunately the implicated vessel was not detectable by MRA.

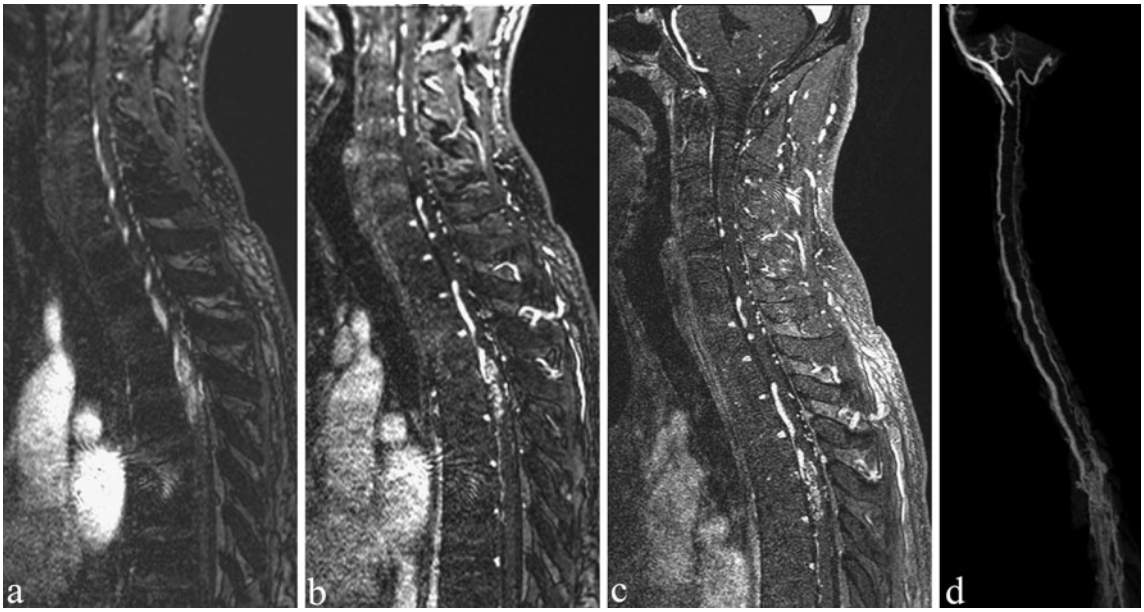

Fig. 1 A 29-year-old man with AVM: dynamic MRA, arterial-phase (**a**), venous-phase (**b**) and high-resolution images (**c**) with 3D reconstructions (**d**)

Discussion

The main advantage of spinal MRA is a better image quality and resolution, which improves the visualization of small-size vessels. The utilization of high vascular remanence contrast agent permits visualization of the arterial and venous phases as well as to obtain high-resolution late enhanced 3D gradient echo MR images.

Currently we could detect both the normal arteries (i.e. the AKA, Fig. 2) and the abnormal vessels as in the prior studies realized at 1.5 Tesla [5, 6]. While the "gold standard" for the evaluation of spinal vessels is conventional angiography, this procedure is still accompanied by risks and requires experience to perform. Dynamic MRA avoids an unnecessary angiography with superselective injections at numerous levels in the case, for example,

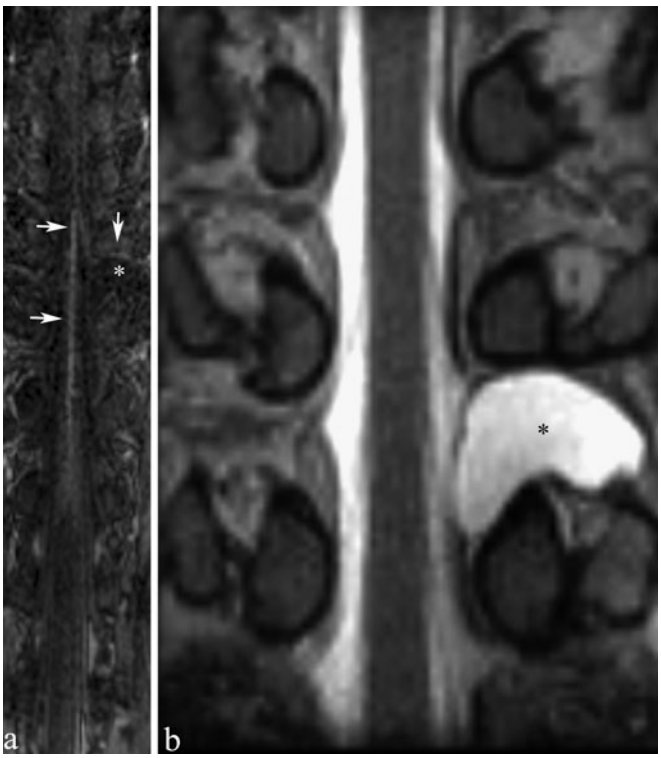

Fig. 2 A 30-year-old woman: the MRA shows clearly an AKA (*arrows*, **a**) passing over the cyst (*asterisk*, **a**, **b**)

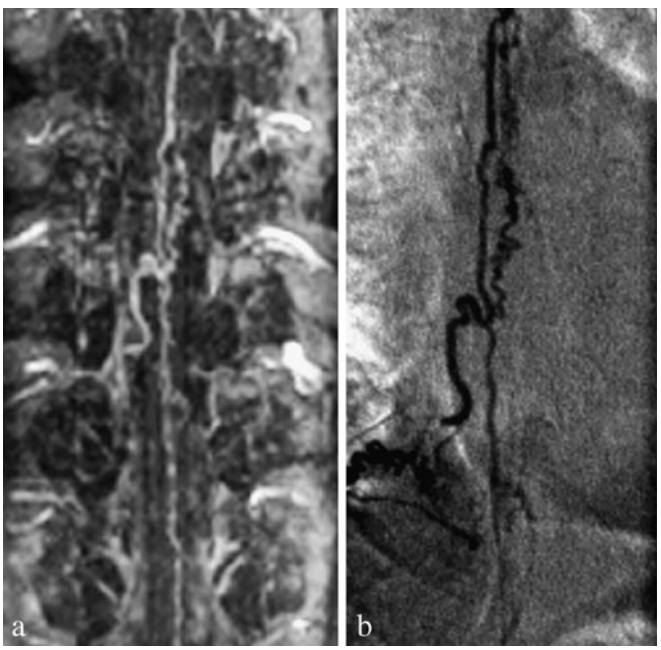

Fig. 3 A 57-year-old man with a dural fistula at the level of Th9 right illustrated by MRA (**a**) and angiography (**b**)

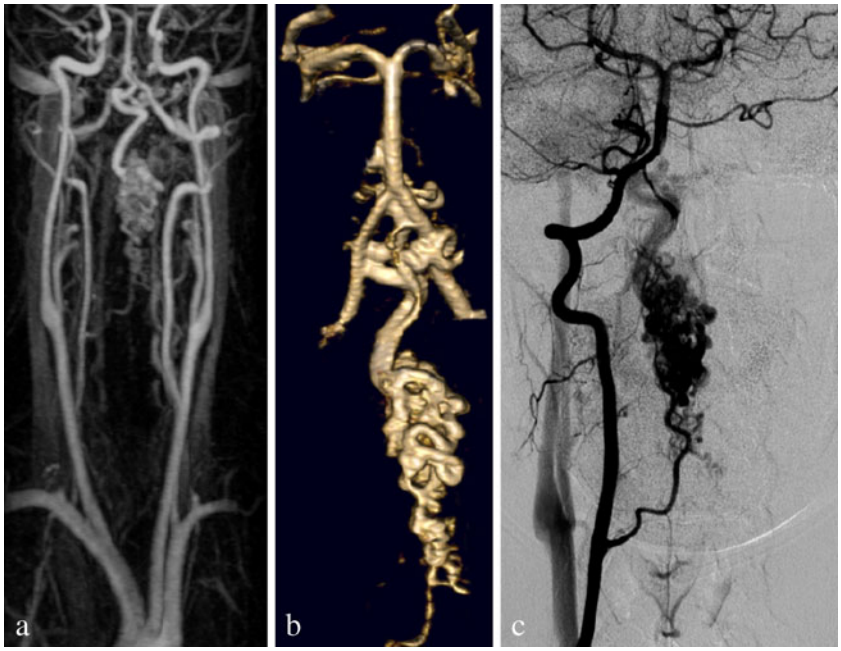

Fig. 4 A 26-year-old woman with a cervical AVM: the MRA (**a**) showing the feeder, nicely demonstrated in the 3D reconstruction (**b**), corresponding to what is seen on DSA (**c**)

where a dural fistula (Fig. 3) or an AVM (Fig. 4) are suspected [7–9]. Usually in our hospital, only the overlying and underlying segments are catheterized for the study of eventual feeder arteries. Krings [10] recommended the utilization of sequences such as CISS 3D or FIESTA, but the problem with these sequences is that differentiation between the veins and the arteries is not possible. When the localization of AKAs is necessary for the surgery of tumours or in the case of aortic aneurysm [11, 12] we avoid the risk of plaque embolization by not performing conventional angiography.

The real advantage of 3D dynamic vascular sequences is the capacity to non-invasively evaluate the shunt location which is extremely helpful to guide invasive conventional angiography [2]. Bowen and Kochan [13] described in 1995 that spinal contrast-enhanced MRA has greatly contributed to localizing these lesions and helping to avoid unnecessary multiple superselective injections; the drawback of the technique used by this author is the non-utilization of the dynamic phase component essential for the classification and subsequent treatment of the vascular malformations.

Recent technical improvements in contrast-enhanced MRA ,such as the use of SENSE or other parallel imaging techniques at 3 T, have allowed to greatly accelerate imaging, thus obtaining both a high spatial and temporal resolution [7, 9]; this can help to better depict feeding arteries as well as anatomy and flow velocity of early venous drainage, thus allowing improved classification of vascular malformations. Also, due to the high resolution of the technique, in the case with a very small structure such as a spinal cord cavernoma, the combination of MR and MRA allowed to help exclude another kind of vascular malformation.

Finally MIP and MPR reconstructions are crucial for the detection and analysis of the vascular malformation; for this purpose it is necessary for the physician to be trained in this kind of reconstruction.

Conclusion

Currently, MRA can provide the exact localization of a vascular malformation and AKA, and thus help detect and characterize spinal vascular lesions before conventional angiography for the diagnosis, thus avoiding an unnecessary intervention and decreasing the risk of embolism or dissections. Standard angiography should be used only for therapeutic purposes.

References

1. Lazorthes G (1983) Le systéme nerveux central, 3 edn. Masson, Paris, p 35
2. Backes W, Nijenhuis R (2008) Advances in spinal cord MR angiography. AJNR Am J Neuroradiol 29:619–631
3. Vargas MI, Delavelle J, Kohler R, Becker C, Lovblad K (2009) Brain and spine MRI artifacts at 3Tesla. J Neuroradiol 2:74–81
4. Vargas MI, Delavelle J, Jlassi H et al (2008) Clinical applications of diffusion tensor tractography of the spinal cord. Neuroradiology 50:25–29
5. Mull M, Nijenhuis R, Backes W, Krings T, Wilmink J, Thron A (2007) Value and limitations of contrast-enhanced MR angiography in spinal arteriovenous malformations and dural arteriovenous fistulas. AJNR Am J Neuroradiol 7:1249–1258

6. Hyodoh H, Shirase R, Kawaharada N et al (2009) MR angiography for detecting the artery of Adamkiewicz and its branching level from the aorta. Magn Reson Med Sci 8:159–164
7. Petkova M, Gauvrit J, Trystram D et al (2009) Three-dimensional dynamic time-resolved contrast-enhanced MRA using parallel imaging and a variable rate k-space sampling strategy in intracranial arteriovenous malformations. J Magn Reson Imaging 29:7–12
8. Parmar H, Ivancevic M, Dudek N, Gandhi D, Mukherji S (2009) Dynamic MRA with four-dimensional time-resolved angiography using keyhole at 3 Tesla in head and neck vascular lesions. J Neuroophthalmol 29:119–127
9. Willinek W, Hadizadeh D, Von Falkenhausen M et al (2008) 4D time-resolved MR angiography with keyhole (4D-TRAK): more than 60 times accelerated MRA using a combination of CENTRA, keyhole, and SENSE at 3.0 T. J Magn Reson Imaging 27:1455–1460
10. Krings T, Geibprasert S (2009) Spinal dural arteriovenous fistulas. AJNR Am J Neuroradiol 4:639–648
11. Nijenhuis RJ, Leiner T, Cornips EM et al (2004) Spinal cord feeding arteries at MR angiography for thoracoscopic spinal surgery: feasibility study and implications for surgical approach. Radiology 2:541–547
12. Kunihiro Y, Hiroyuki N, Atsushi O et al (2003) MR angiography and CT angiography of the artery of Adamkiewicz: noninvasive preoperative assessment of thoracoabdominal aortic aneurysm. Radiographics 23:1215–1225
13. Bowen B, Fraser K, Kochan J (1995) Spinal dural arteriovenous fistulas: evaluation with MR angiography. AJNR Am J Neuroradiol 16:2029–2043